Relativistic many-body calculations of electric-dipole transitions between $n=2$ states in B-like ions

U. I. Safronova, W. R. Johnson, and A. E. Livingston

Department of Physics, University of Notre Dame, Notre Dame, Indiana 46556

(Received 25 February 1999; revised manuscript received 15 April 1999)

Transition rates, oscillator strengths, and line strengths are calculated for the 49 possible electric-dipole transitions between the eight even-parity $2s2p^2$ states and the seven odd-parity $2s^2 2p$ and $2p^3$ states in boronlike ions with nuclear charges ranging from $Z=6$ to 100. Relativistic many-body perturbation theory (MBPT), including the Breit interaction, is used to evaluate retarded E_1 matrix elements in length and velocity forms. The calculations start from a $1s^2$ Dirac-Fock potential. First-order MBPT is used to obtain intermediate coupling coefficients and second-order MBPT is used to calculate transition matrix elements. Contributions from negative-energy states are included in the second-order E_1 matrix elements to ensure gauge independence of transition amplitudes. The transition energies used in the calculation of oscillator strengths and transition rates are from second-order MBPT. Transition rates, line strengths, and oscillator strengths are compared with critically evaluated experimental values and with results from other recent calculations. Lifetimes of the five possible odd-parity upper levels and the five possible even-parity upper levels are given for $Z=6-100$. Trends of the transition rates as functions of Z are illustrated graphically for selected transitions. [S1050-2947(99)06808-0]

PACS number(s): 32.70.Cs, 31.25.Eb, 31.25.Jf, 31.30.Jv

I. INTRODUCTION

Many theoretical studies of transitions in B-like ions have been made during the past 30–40 years, especially for electric-dipole transitions within the $n=2$ complex of states. Transition rates and oscillator strengths for B-like ions have been calculated using Z-expansion [1–5], configuration interaction (CI) [6–15], multiconfiguration Hartree-Fock (MCHF) [16–25], R-matrix [26,27], model potential [28–31], and multiconfiguration Dirac-Fock (MCDF) [32–34] methods. A correspondingly large number of experimental studies of the lifetimes of $n=2$ states have been made using beam foil techniques. Most of these investigations concerned low-Z ions: N^{2+} [35–42], O^{3+} [40,43–45], F^{4+} [46], Ne^{5+} [47–49], and Na^{6+} [50]. Lifetime measurements for the high-Z ions Si^{9+} [51,52], P^{10+} [53], S^{11+} [54,55], and Cl^{12+} [56–58] have also been reported. A critical data compilation based on available theoretical and experimental sources was given by Wiese, Fuhr, and Deters [59] for B-like carbon, nitrogen, and oxygen. Critical data compilations for high-Z boronlike ions are given in [60–65].

In the present paper, relativistic many-body perturbation theory (MBPT) is used to determine matrix elements, oscillator strengths, and transition rates for all allowed and forbidden electric-dipole transitions within the $n=2$ complex of states in boronlike ions with nuclear charges ranging from $Z=6$ to 100. Retarded E_1 matrix elements are evaluated in both length and velocity forms. These calculations start from a $1s^2$ Dirac-Fock potential. First-order perturbation theory is used to obtain intermediate coupling coefficients and second-order MBPT is used to determine transition matrix elements. Contributions from negative-energy states are included in the second-order E_1 matrix elements to ensure agreement between length-form and velocity-form amplitudes. The transi-

tion energies used in the calculation of oscillator strengths and transition rates are obtained from second-order MBPT.

The present data, which are in fair agreement with critically evaluated data for low-Z ions, increase in accuracy with increasing Z. Our data are in good agreement with R-matrix calculations [27] for low Z and in fair agreement with MCDF calculations [32] for high Z. Our predicted lifetimes agree with all available experimental values to within one or two times the estimated experimental errors. We believe that the present data are more accurate than other available experimental or theoretical data for intermediate and high-Z ions, $Z \gtrsim 10$.

II. METHOD

The evaluation of the first- and second-order reduced dipole matrix elements $Z^{(1)}$ and $Z^{(2)}$ for boronlike ions follows the pattern of the corresponding calculation for berylliumlike ions given in Ref. [66]. We use the second-order one- and two-particle matrix elements for berylliumlike ions calculated in [66], but recoupled as described in the Appendix, to obtain the contributions from first- and second-order perturbation theory; the reader is referred to [66] for a discussion of how the basic one- and two-particle matrix elements were evaluated. It should be noted that the uncoupled one- and two-particle matrix elements calculated in [66] are the only data needed in the present second-order MBPT calculation. This is in contrast to calculations of the second-order energy $E^{(2)}$ for systems with three valence electrons, where additional three-particle diagrams must be evaluated [67].

The model space for the $n=2$ complex in boronlike ions has seven odd-parity states and eight even-parity states. These states are summarized in Table I, where both jj and LS designations are given. When starting calculations from relativistic Dirac-Fock wave functions, it is natural to use the

TABLE I. Possible three-particle states in the $n=2$ complex.

	Even-parity states			Odd-parity states	
J	jj coupling	LS coupling	J	jj coupling	LS coupling
1/2	$2p_{1/2}2p_{1/2}[0]2s_{1/2}$	$2s2p^2\ ^4P$	1/2	$2s_{1/2}2s_{1/2}[0]2p_{1/2}$	$2s^22p\ ^2P$
1/2	$2p_{1/2}2p_{3/2}[1]2s_{1/2}$	$2s2p^2\ ^2S$	1/2	$2p_{3/2}2p_{3/2}[0]2p_{1/2}$	$2p^3\ ^2P$
1/2	$2p_{3/2}2p_{3/2}[0]2s_{1/2}$	$2s2p^2\ ^2P$			
3/2	$2p_{1/2}2p_{3/2}[1]2s_{1/2}$	$2s2p^2\ ^4P$	3/2	$2s_{1/2}2s_{1/2}[0]2p_{3/2}$	$2s^22p\ ^2P$
3/2	$2p_{1/2}2p_{3/2}[2]2s_{1/2}$	$2s2p^2\ ^2D$	3/2	$2p_{1/2}2p_{1/2}[0]2p_{3/2}$	$2p^3\ ^4S$
3/2	$2p_{3/2}2p_{3/2}[2]2s_{1/2}$	$2s2p^2\ ^2P$	3/2	$2p_{3/2}2p_{3/2}[2]2p_{1/2}$	$2p^3\ ^2D$
			3/2	$2p_{3/2}2p_{3/2}[0]2p_{3/2}$	$2p^3\ ^2P$
5/2	$2p_{1/2}2p_{3/2}[2]2s_{1/2}$	$2s2p^2\ ^4P$	5/2	$2p_{3/2}2p_{3/2}[2]2p_{1/2}$	$2p^3\ ^2D$
5/2	$2p_{3/2}2p_{3/2}[2]2s_{1/2}$	$2s2p^2\ ^2D$			

jj designations for uncoupled transition and energy matrix elements; however, neither jj nor LS coupling describes *physical* states properly, except for unique states such as $2p^3\ ^2D_{5/2}\equiv 2p_{3/2}2p_{3/2}[2]2p_{1/2}[5/2]$.

In Table II, we list values of *uncoupled* first- and second-order dipole matrix elements $Z^{(1)}$ and $Z^{(2)}$, together with derivative terms $P^{(\mathrm{derv})}$ for B-like iron, $Z=26$. For simplicity, we only list values for the six possible transitions between even- and odd-parity three-particle states with $J=1/2$. The derivative terms shown in Table II arise because transition amplitudes depend on energy, and the transition energy changes order-by-order in MBPT calculations. Both length and velocity forms are given for the matrix elements. We can see that the first-order matrix elements $Z_L^{(1)}$ and $Z_V^{(1)}$ differ by 10–20 %; the $L-V$ differences between second-order matrix elements are much larger as seen by comparing $Z_L^{(2)}$ and $Z_V^{(2)}$. Physical two-particle states are linear combinations of uncoupled three-particle states (vwu) in the model space; correspondingly, transition amplitudes between physical states are linear combinations of the uncoupled transition matrix elements such as those given in Table II. The expansion coefficients and energies are obtained by diagonalizing the effective Hamiltonian as discussed in [67]. In the last paragraph of the Appendix, we give a detailed explanation of how the uncoupled matrix elements listed in Table II are combined to give coupled matrix elements between physical states.

In Table III, we present values of *coupled* reduced matrix elements in length L and velocity V forms for the six 1/2-1/2 transitions considered in Table II. Although we use an intermediate-coupling scheme, it is nevertheless convenient to label the physical states using the LS scheme. We see that the coupled matrix elements in Table III differ in L and V

forms only in the fourth or fifth digits. These $L-V$ differences arise because we start our MBPT calculations using a nonlocal Dirac-Fock (DF) potential. If we were to replace the DF potential by a local potential, the $L-V$ differences would disappear completely.

It should be emphasized that we include negative energy state (NES) contributions to sums over intermediate states. Ignoring these NES contributions leads to small changes in the L-form matrix elements but substantial changes in some of the V-form matrix elements, with a consequent loss of gauge independence. We find that negative energy states contribute from 1% to 3% to the V-form matrix elements for B-like iron shown in Table III. The NES contributions to V-form matrix elements become larger for small Z, especially for transitions with $\Delta S=1$, where they can contribute as much as 30%.

III. RESULTS AND DISCUSSION

In Table IV, we compare our results for transition rates $A(s^{-1})$, oscillator strengths f, and line strengths S (a.u.) of LS-allowed transitions in N^{2+} with recommended data from the National Institute for Standards and Technology [59]. In view of the gauge independence discussed above, our results are presented in L form only. Uncertainties in the recommended values given in [59] were estimated to be less than 10% based on comparisons with experimental results from lifetime and emission measurements. The agreement between theoretical L-form and V-form theoretical results was also used in [59] as an indicator of accuracy. Our theoretical results are seen to agree with the recommended data for the low-Z ion N^{2+} at the 10–30 % level. Since the present transition data are obtained using a single method for all Z and

TABLE II. Uncoupled reduced matrix elements in length L and velocity V forms for 1/2-1/2 transitions in Fe^{+21}. Notation: $2p=2p_{3/2}$, $2p^*=2p_{1/2}$.

$vw[J_{12}]u(J)$	$v'w'[J'_{12}]u'(J')$	$Z_L^{(1)}$	$Z_V^{(1)}$	$Z_L^{(2)}$	$Z_V^{(2)}$	$P_L^{(\mathrm{derv})}$	$P_V^{(\mathrm{derv})}$
$2s2s[0]2p^*(1/2)$	$2p^*2p^*[0]2s(1/2)$	0.172296	0.188645	0.002029	0.153062	0.172301	0.000011
$2s2s[0]2p^*(1/2)$	$2p^*2p[1]2s(1/2)$	0.200524	0.214544	0.003836	0.071886	0.200513	−0.000022
$2s2s[0]2p^*(1/2)$	$2p2p[0]2s(1/2)$	0.000000	0.000000	−0.001756	0.053360	0.000000	0.000000
$2p2p[0]2p^*(1/2)$	$2p^*2p^*[0]2s(1/2)$	0.000000	0.000000	0.001756	−0.053360	0.000000	0.000000
$2p2p[0]2p^*(1/2)$	$2p^*2p[1]2s(1/2)$	−0.141792	−0.151705	0.001296	−0.107793	−0.141784	0.000015
$2p2p[0]2p^*(1/2)$	$2p2p[0]2s(1/2)$	0.172296	0.188645	0.000884	0.051734	0.172301	0.000011

TABLE III. Coupled reduced matrix elements in length L and velocity V forms for Fe^{+21}.

$vwu(^{2S+1}L_J)$	$v'w'u'(^{2S'+1}L'_{J'})$	L	V
$2s^22p(^2P_{1/2})$	$2s2p^2(^4P_{1/2})$	0.032485	0.032482
$2s^22p(^2P_{1/2})$	$2s2p^2(^2S_{1/2})$	0.241795	0.241863
$2s^22p(^2P_{1/2})$	$2s2p^2(^2P_{1/2})$	0.051049	0.051056
$2p^3(^2P_{1/2})$	$2s2p^2(^4P_{1/2})$	0.011294	0.011292
$2p^3(^2P_{1/2})$	$2s2p^2(^2S_{1/2})$	−0.078174	−0.078150
$2p^3(^2P_{1/2})$	$2s2p^2(^2P_{1/2})$	−0.227479	−0.227330

are expected to improve in accuracy with increasing Z, we expect that our data for high Z will also be reliable.

In Table V, we present theoretical transition data for all 49 transitions in two high-Z ions, Fe^{+21} and Xe^{49+}. The data for Fe^{+21} agree with the recommended values from Ref. [64] to better than 10% for LS-allowed transitions and to 10–30 % for LS-forbidden transitions. We expect our values to be more accurate than the data from [64] for both allowed and forbidden transitions, since Coulomb and Breit correlation corrections are included in our calculations as well as retardation.

Results of the present calculations for lifetimes τ (ps) of five even-parity $2s2p^2$ levels and five odd-parity $2p^3$ levels in B-like ions with $Z=6$–100, obtained by summing E_1

transitions rates from each level to all possible lower levels, can be found in Table I of the E-PAPS file [69]. Contributions of different decay channels for $2p^3$ $^2D_{5/2}$ and $2p^3$ $^2D_{3/2}$ levels are shown in Figs. 1 and 2. We see that LS-allowed transitions give the largest contribution to the rates for Z up to 25. Contributions from LS-forbidden transitions compete with strongest allowed rates for higher values of Z. Our lifetime data are compared with experimental measurements for ions with $Z=7$–10 in Table VI and $Z=14$–17 in Table VII. In both ranges of Z, our theoretical lifetimes agree with measured lifetimes to within one or two times the experimental error limits.

It is of some interest to consider theoretical rates A_J for $2s^22p$ ^2P_J–$2s2p^2$ $^2S_{1/2}$ and $2s^22p$ ^2P_J–$2s2p^2$ $^2P_{1/2}$ tran-

TABLE IV. Transition energies E (cm^{-1}), wavelengths λ (Å), line strengths S (a.u.), oscillator strengths f, and rates A (s^{-1}) in N^{2+} ($Z=7$). The superscript r designates recommended data from [59]. The number in brackets represents the power of 10.

| Down level	Upper level	E	λ	A	A^r	f	f^r	S	S^r
$2s^22p(^2P_{1/2})$	$2s2p^2(^2S_{1/2})$	131688	759.37	8.26[8]	9.58[8]	7.15[−2]	8.37[−2]	3.57[−1]	4.21[−1]
$2s^22p(^2P_{3/2})$	$2s2p^2(^2S_{1/2})$	131512	760.39	1.85[9]	1.61[9]	7.00[−2]	8.10[−2]	7.01[−1]	8.15[−1]
$2s^22p(^2P_{1/2})$	$2s2p^2(^2P_{1/2})$	144248	693.25	2.96[9]	3.83[9]	2.13[−1]	2.70[−1]	9.73[−1]	1.22
$2s^22p(^2P_{1/2})$	$2s2p^2(^2P_{3/2})$	144363	692.70	7.43[8]	9.63[8]	1.07[−1]	1.36[−1]	4.88[−1]	6.11[−1]
$2s^22p(^2P_{3/2})$	$2s2p^2(^2P_{1/2})$	144071	694.10	1.49[9]	1.95[9]	5.40[−2]	6.88[−2]	4.93[−1]	6.22[−1]
$2s^22p(^2P_{3/2})$	$2s2p^2(^2P_{3/2})$	144186	693.55	3.71[9]	4.54[9]	2.68[−1]	3.20[−1]	2.44	2.89
$2s^22p(^2P_{1/2})$	$2s2p^2(^2D_{3/2})$	100019	999.81	3.94[8]	4.18[8]	1.18[−1]	1.23[−1]	7.79[−1]	8.00[−1]
$2s^22p(^2P_{3/2})$	$2s2p^2(^2D_{3/2})$	99842	1001.58	7.77[7]	8.17[7]	1.17[−2]	1.20[−2]	1.54[−1]	1.57[−1]
$2s^22p(^2P_{3/2})$	$2s2p^2(^2D_{5/2})$	99836	1001.64	4.70[8]	4.97[8]	1.10[−1]	1.06[−1]	1.40	1.43
$2s2p^2(^4P_{1/2})$	$2p^3(^4S_{3/2})$	129151	774.29	7.55[8]	8.19[8]	1.36[−1]	1.46[−1]	6.92[−1]	7.42[−1]
$2s2p^2(^4P_{3/2})$	$2p^3(^4S_{3/2})$	129089	774.66	1.51[9]	1.64[9]	1.36[−1]	1.46[−1]	1.38	1.48
$2s2p^2(^4P_{5/2})$	$2p^3(^4S_{3/2})$	129001	775.19	2.26[9]	2.45[9]	1.36[−1]	1.46[−1]	2.08	2.23
$2s2p^2(^2D_{3/2})$	$2p^3(^2D_{3/2})$	101498	985.24	9.56[8]	8.84[8]	1.39[−1]	1.27[−1]	1.81	1.64
$2s2p^2(^2D_{3/2})$	$2p^3(^2D_{5/2})$	101487	985.34	7.17[7]	6.66[7]	1.57[−2]	1.44[−2]	2.03[−1]	1.86[−1]
$2s2p^2(^2D_{5/2})$	$2p^3(^2D_{3/2})$	101504	985.18	1.08[8]	1.02[8]	1.05[−2]	9.74[−3]	2.04[−1]	1.89[−1]
$2s2p^2(^2D_{5/2})$	$2p^3(^2D_{5/2})$	101493	985.29	9.94[8]	9.21[8]	1.45[−1]	1.33[−1]	2.82	2.57
$2s2p^2(^2D_{3/2})$	$2p^3(^2P_{1/2})$	129265	773.60	1.94[9]	2.34[9]	8.69[−2]	1.05[−1]	8.85[−1]	1.06
$2s2p^2(^2D_{3/2})$	$2p^3(^2P_{3/2})$	129271	773.57	1.95[8]	2.36[8]	1.75[−2]	2.11[−2]	1.78[−1]	2.15[−1]
$2s2p^2(^2D_{5/2})$	$2p^3(^2P_{3/2})$	129277	773.53	1.74[9]	2.09[9]	1.04[−1]	1.25[−1]	1.59	1.91
$2s2p^2(^2S_{1/2})$	$2p^3(^2P_{1/2})$	97596	1024.64	2.89[8]	2.48[8]	4.55[−2]	3.76[−2]	3.07[−1]	2.49[−1]
$2s2p^2(^2S_{1/2})$	$2p^3(^2P_{3/2})$	97602	1024.57	2.96[8]	2.57[8]	9.31[−2]	7.80[−2]	6.28[−1]	5.16[−1]
$2s2p^2(^2P_{1/2})$	$2p^3(^2P_{1/2})$	85036	1175.97	5.91[8]	5.87[8]	1.23[−1]	1.23[−1]	9.49[−1]	9.59[−1]
$2s2p^2(^2P_{1/2})$	$2p^3(^2P_{3/2})$	85042	1175.88	1.44[8]	1.42[8]	5.99[−2]	5.95[−2]	4.64[−1]	4.63[−1]
$2s2p^2(^2P_{3/2})$	$2p^3(^2P_{1/2})$	84921	1177.56	2.92[8]	2.89[8]	3.04[−2]	3.04[−2]	4.71[−1]	4.74[−1]
$2s2p^2(^2P_{3/2})$	$2p^3(^2P_{3/2})$	84927	1177.48	7.34[8]	7.29[8]	1.53[−1]	1.53[−1]	2.37	2.39
$2s2p^2(^2P_{1/2})$	$2p^3(^2D_{3/2})$	57269	1746.14	1.37[8]	1.28[8]	1.25[−1]	1.17[−1]	1.44	1.34
$2s2p^2(^2P_{3/2})$	$2p^3(^2D_{3/2})$	57154	1749.66	2.69[7]	2.48[7]	1.23[−2]	1.14[−2]	2.85[−1]	2.62[−1]
$2s2p^2(^2P_{3/2})$	$2p^3(^2D_{5/2})$	57143	1749.99	1.63[8]	1.51[8]	1.12[−1]	1.04[−1]	2.59	2.40

TABLE V. Wavelengths λ (Å), line strengths S (a.u.), oscillator strengths f, and transition probabilities A (s^{-1}) for Fe^{+21} and Xe^{+49}. The number in brackets represents the power of 10.

| | | Fe^{+21} (Z=26) | | | | Xe^{+49} (Z=54) | | | |
Lower level	Upper level	λ	S	f	A	λ	S	f	A
$2s^22p(^2P_{1/2})$	$2s2p^2(^4P_{1/2})$	247.19	1.06[−3]	6.48[−4]	7.07[7]	75.99	3.96[−3]	7.91[−3]	9.13[9]
$2s^22p(^2P_{1/2})$	$2s2p^2(^4P_{3/2})$	217.29	3.65[−5]	2.55[−5]	1.80[6]	26.26	1.13[−4]	6.54[−4]	3.16[9]
$2s^22p(^2P_{3/2})$	$2s2p^2(^4P_{1/2})$	349.31	5.32[−4]	1.16[−4]	1.26[7]	63.53	2.29[−4]	5.48[−4]	4.53[8]
$2s^22p(^2P_{3/2})$	$2s2p^2(^4P_{3/2})$	292.44	3.41[−4]	8.86[−5]	6.91[6]	108.89	9.31[−4]	6.49[−4]	3.65[8]
$2s^22p(^2P_{3/2})$	$2s2p^2(^4P_{5/2})$	253.12	2.93[−3]	8.78[−4]	6.09[7]	85.22	7.47[−3]	6.65[−3]	4.07[9]
$2s^22p(^2P_{1/2})$	$2s2p^2(^2S_{1/2})$	117.19	5.85[−2]	7.58[−2]	3.68[10]	22.38	9.59[−3]	6.51[−2]	8.67[11]
$2s^22p(^2P_{3/2})$	$2s2p^2(^2S_{1/2})$	136.05	5.07[−5]	2.83[−5]	2.04[7]	63.33	2.08[−3]	2.49[−3]	8.29[9]
$2s^22p(^2P_{1/2})$	$2s2p^2(^2P_{1/2})$	102.23	2.61[−3]	3.87[−3]	2.47[9]	13.44	6.06[−7]	6.84[−6]	2.52[8]
$2s^22p(^2P_{1/2})$	$2s2p^2(^2P_{3/2})$	100.82	1.24[−2]	1.87[−2]	6.13[9]	13.43	8.80[−5]	9.95[−4]	1.84[10]
$2s^22p(^2P_{3/2})$	$2s2p^2(^2P_{1/2})$	116.29	5.13[−2]	3.35[−2]	3.30[10]	21.99	7.53[−3]	2.60[−2]	7.17[11]
$2s^22p(^2P_{3/2})$	$2s2p^2(^2P_{3/2})$	114.47	1.26[−1]	8.35[−2]	4.25[10]	21.95	2.53[−2]	8.75[−2]	1.21[12]
$2s^22p(^2P_{1/2})$	$2s2p^2(^2D_{3/2})$	135.87	5.17[−2]	5.78[−2]	1.04[10]	22.39	1.52[−2]	1.03[−1]	6.87[11]
$2s^22p(^2P_{3/2})$	$2s2p^2(^2D_{3/2})$	161.88	3.65[−4]	1.71[−4]	4.35[7]	63.41	2.78[−3]	3.32[−3]	5.51[9]
$2s^22p(^2P_{3/2})$	$2s2p^2(^2D_{5/2})$	156.09	6.60[−2]	3.21[−2]	5.86[9]	25.29	7.27[−3]	2.18[−2]	1.52[11]
$2s2p^2(^4P_{1/2})$	$2p^3(^4S_{3/2})$	117.52	3.15[−2]	4.07[−2]	9.83[9]	21.93	1.04[−2]	7.21[−2]	5.00[11]
$2s2p^2(^4P_{3/2})$	$2p^3(^4S_{3/2})$	125.75	5.74[−2]	3.46[−2]	1.46[10]	48.37	3.28[−3]	5.15[−3]	1.47[10]
$2s2p^2(^4P_{5/2})$	$2p^3(^4S_{3/2})$	134.75	8.99[−2]	3.38[−2]	1.86[10]	55.18	1.44[−2]	1.32[−2]	4.33[10]
$2s2p^2(^4P_{1/2})$	$2p^3(^2D_{3/2})$	100.94	3.58[−5]	5.38[−5]	1.76[7]	13.90	7.86[−5]	8.58[−4]	1.48[10]
$2s2p^2(^4P_{3/2})$	$2p^3(^2D_{3/2})$	106.95	4.29[−3]	3.05[−3]	1.78[9]	21.27	1.08[−2]	3.84[−2]	5.66[11]
$2s2p^2(^4P_{3/2})$	$2p^3(^2D_{5/2})$	103.59	1.29[−4]	9.49[−5]	3.93[7]	20.58	2.66[−4]	9.81[−4]	1.03[10]
$2s2p^2(^4P_{5/2})$	$2p^3(^2D_{3/2})$	113.39	3.90[−4]	1.74[−4]	1.35[8]	22.49	1.55[−3]	3.49[−3]	6.90[10]
$2s2p^2(^4P_{5/2})$	$2p^3(^2D_{5/2})$	109.62	6.48[−3]	2.99[−3]	1.66[9]	21.71	1.50[−2]	3.50[−2]	4.95[11]
$2s2p^2(^4P_{1/2})$	$2p^3(^2P_{1/2})$	85.88	1.28[−4]	2.26[−4]	2.04[8]	13.05	1.71[−6]	1.99[−5]	7.79[8]
$2s2p^2(^4P_{1/2})$	$2p^3(^2P_{3/2})$	81.81	3.75[−6]	6.96[−6]	3.47[6]	9.66	5.64[−9]	8.87[−8]	3.16[6]
$2s2p^2(^4P_{3/2})$	$2p^3(^2P_{1/2})$	90.20	3.25[−5]	2.74[−5]	4.49[7]	19.35	7.20[−5]	2.83[−4]	1.01[10]
$2s2p^2(^4P_{3/2})$	$2p^3(^2P_{3/2})$	85.71	3.32[−4]	2.94[−4]	2.67[8]	12.73	1.71[−5]	1.02[−4]	4.19[9]
$2s2p^2(^4P_{5/2})$	$2p^3(^2P_{3/2})$	89.80	1.79[−4]	1.01[−4]	1.25[8]	13.16	2.79[−6]	1.07[−5]	6.19[8]
$2s2p^2(^2D_{3/2})$	$2p^3(^4S_{3/2})$	192.50	1.44[−3]	5.69[−4]	1.02[8]	70.98	6.05[−3]	6.48[−3]	8.57[9]
$2s2p^2(^2D_{5/2})$	$2p^3(^4S_{3/2})$	201.39	1.37[−4]	3.45[−5]	8.51[6]	103.26	1.53[−4]	1.13[−4]	4.71[7]
$2s2p^2(^2D_{3/2})$	$2p^3(^2D_{3/2})$	151.69	5.02[−2]	2.52[−2]	7.29[9]	24.73	1.99[−3]	6.12[−3]	6.67[10]
$2s2p^2(^2D_{3/2})$	$2p^3(^2D_{5/2})$	145.02	2.90[−2]	1.52[−2]	3.21[9]	23.80	1.72[−2]	5.49[−2]	4.30[11]
$2s2p^2(^2D_{5/2})$	$2p^3(^2D_{3/2})$	157.16	3.48[−2]	1.12[−2]	4.53[9]	60.02	9.24[−3]	7.79[−3]	2.16[10]
$2s2p^2(^2D_{5/2})$	$2p^3(^2D_{5/2})$	150.01	1.21[−1]	4.09[−2]	1.21[10]	54.82	1.07[−2]	9.91[−3]	2.20[10]
$2s2p^2(^2D_{3/2})$	$2p^3(^2P_{1/2})$	120.06	4.64[−2]	2.94[−2]	2.72[10]	22.17	9.56[−3]	3.28[−2]	8.88[11]
$2s2p^2(^2D_{3/2})$	$2p^3(^2P_{3/2})$	112.24	1.33[−2]	9.01[−3]	4.77[9]	13.90	8.63[−5]	4.72[−4]	1.63[10]
$2s2p^2(^2D_{5/2})$	$2p^3(^2P_{3/2})$	115.21	4.07[−2]	1.79[−2]	1.35[10]	20.75	6.27[−3]	1.53[−2]	3.55[11]
$2s2p^2(^2S_{1/2})$	$2p^3(^4S_{3/2})$	248.65	2.82[−3]	1.72[−3]	9.29[7]	71.08	5.88[−3]	1.26[−2]	8.29[9]
$2s2p^2(^2S_{1/2})$	$2p^3(^2D_{3/2})$	184.53	7.55[−2]	6.21[−2]	6.08[9]	24.74	1.11[−2]	6.80[−2]	3.70[11]
$2s2p^2(^2S_{1/2})$	$2p^3(^2P_{1/2})$	139.74	6.11[−3]	6.64[−3]	2.27[9]	22.18	3.91[−3]	2.68[−2]	3.63[11]
$2s2p^2(^2S_{1/2})$	$2p^3(^2P_{3/2})$	129.26	1.59[−2]	1.87[−2]	3.73[9]	13.90	6.36[−5]	6.94[−4]	1.20[10]
$2s2p^2(^2P_{1/2})$	$2p^3(^4S_{3/2})$	360.60	8.62[−4]	3.63[−4]	9.30[6]	64.00	1.70[−4]	8.08[−4]	1.64[8]
$2s2p^2(^2P_{3/2})$	$2p^3(^4S_{3/2})$	379.35	2.80[−3]	5.60[−4]	2.59[7]	63.66	5.39[−4]	6.43[−4]	1.06[9]
$2s2p^2(^2P_{1/2})$	$2p^3(^2P_{1/2})$	169.27	5.17[−2]	4.64[−2]	1.08[10]	64.97	6.68[−3]	1.56[−2]	2.47[10]
$2s2p^2(^2P_{1/2})$	$2p^3(^2P_{3/2})$	154.14	1.18[−2]	1.16[−2]	1.63[9]	23.67	5.69[−3]	3.65[−2]	2.17[11]
$2s2p^2(^2P_{3/2})$	$2p^3(^2P_{1/2})$	173.29	1.08[−2]	4.71[−3]	2.09[9]	65.33	4.92[−5]	5.72[−5]	1.79[8]
$2s2p^2(^2P_{3/2})$	$2p^3(^2P_{3/2})$	157.46	1.41[−1]	6.82[−2]	1.83[10]	23.72	2.76[−2]	8.83[−2]	1.05[12]
$2s2p^2(^2P_{1/2})$	$2p^3(^2D_{3/2})$	239.77	2.12[−2]	1.34[−2]	7.78[8]	93.28	4.66[−5]	7.58[−5]	2.91[7]
$2s2p^2(^2P_{3/2})$	$2p^3(^2D_{3/2})$	247.91	1.51[−3]	4.63[−4]	4.49[7]	94.02	2.06[−3]	1.66[−3]	1.25[9]
$2s2p^2(^2P_{3/2})$	$2p^3(^2D_{5/2})$	230.58	1.15[−1]	3.77[−2]	3.15[9]	81.84	1.17[−2]	1.09[−2]	7.22[9]

sitions for $J=1/2$ and 3/2. The branching ratio $A_{3/2}/A_{1/2}$ for the former transition is equal to 2 in the LS-coupling limit, as is the ratio $A_{1/2}/A_{3/2}$ for the latter transition. Deviation of either ratio from 2 indicates the presence of relativistic (spin-orbit) effects. The spin-orb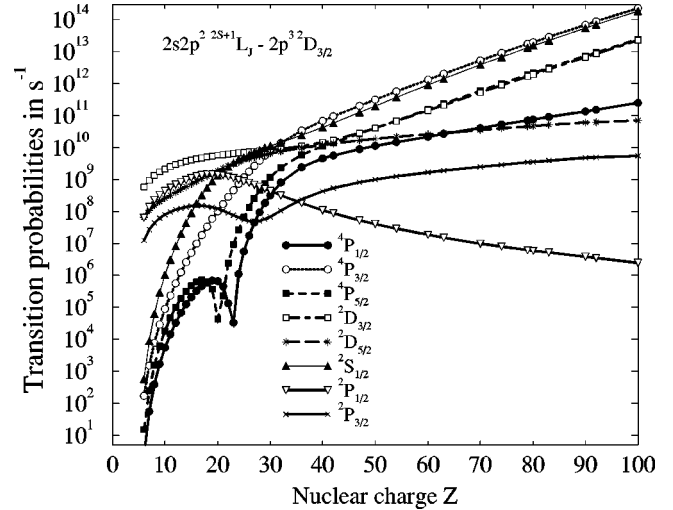it interaction for the $2s2p^2$ $^2S_{1/2}$ and $^2P_{1/2}$ levels was discussed by Dankwort and Trefftz in [20,21]. The model space for even-parity states with $J=1/2$ includes three states: $2p_{1/2}2p_{1/2}[0]2s_{1/2}$, $2p_{1/2}2p_{3/2}[1]2s_{1/2}$, and $2p_{3/2}2p_{3/2}[0]2s_{1/2}$. The strong mixing of $2p_{1/2}2p_{3/2}[1]2s_{1/2}$ and $2p_{3/2}2p_{3/2}[0]2s_{1/2}$ states was
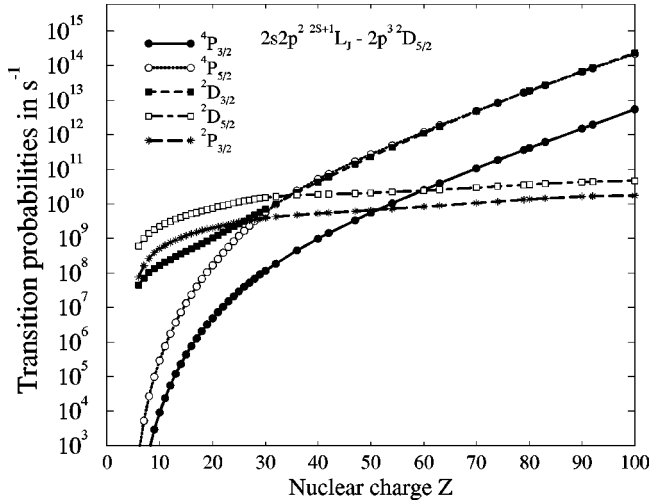
FIG. 1. Rates for $2s2p^2$–$2p^3$ $^2D_{5/2}$ transitions as functions of Z.

FIG. 2. Rates for $2s2p^2$–$2p^3$ $^2D_{3/2}$ transitions as functions of Z.

discussed in Refs. [33] and [67]. In Fig. 3, we compare the experimental data from [68] with our theoretical values. The trend of the experiments follows the theoretical predictions fairly well, but there are substantial deviations from the theory, especially for $Z=15$. It should be noted that the data given in [68] provided the first systematic study of line intensity ratios and served as a probe of intermediate coupling in the B-like system.

Comparison of our calculations of transition rates and oscillator strengths with R-matrix calculations from Ref. [27] and with MCDF calculations from [32] for nine LS-allowed transitions in ions with $Z=9$, 18, and 26 can be found in Table II of the E-PAPS file [69]. For the low-Z ion, our calculations agree fairly well with the R-matrix calculations, which include correlation, but they disagree substantially with the uncorrelated MCDF calculations. As Z increases, the present calculations deviate more and more from the nonrelativistic R-matrix calculations, which assume pure LS coupling. However, with increasing Z, the agreement between our calculations and the MCDF calculations improves, illustrating the diminishing importance of correlation with Z and the increasing importance of relativistic effects. The

present calculations provide a natural way to interpolate between correlated nonrelativistic calculations at low Z and uncorrelated relativistic calculations at high Z.

The general trends of the Z dependence of transition rates are illustrated for the transitions from the five $2s2p^2$ levels into two $2s^22p$ levels in B-like ions in Figs. 4, 5, and 6. We observe strong deviations from LS coupling in all of these figures. For example, the ratio of transition rates $2s^22p$ $^2P_{1/2}$–$2s2p^2$ $^2D_{3/2}$ and $2s^22p$ $^2P_{3/2}$–$2s2p^2$ $^2D_{3/2}$ is predicted to be 5 in LS coupling. From Fig. 6, this prediction is seen to be valid for $Z \lesssim 10$. This and other differences with predictions based on pure LS coupling can be observed in these figures. The sharp features near $Z=25$ in Fig. 4 and $Z=29$ in Fig. 6 are the results of a level crossings.

IV. CONCLUSION

We have presented a systematic second-order relativistic MBPT study of reduced matrix elements, oscillator strengths, and transition rates for $2s$-$2p$ electric dipole transitions in boronlike ions with nuclear charges Z ranging from

TABLE VI. Comparison of theoretical and experimental lifetimes (ns) for B-like ions with $Z=7$–10.

Level	$Z=7$ Present	$Z=7$ Expt.	$Z=8$ Present	$Z=8$ Expt. [a]	$Z=9$ Present	$Z=9$ Expt. [b]	$Z=10$ Present	$Z=10$ Expt. [c]
$2s2p^2(^2P)$	0.225	0.20±0.06 [d]	0.167	0.158±0.007	0.132	0.117±0.05	0.109	0.132±0.005
$2s2p^2(^2S)$	0.411	0.32±0.06 [d]	0.303	0.29±0.02	0.240	0.215±0.02	0.198	0.218±0.010
$2s2p^2(^2D)$	2.12	2.09±0.08 [d]	1.49	1.64±0.08	1.13	1.25±0.10	0.910	0.958±0.025
$2p^3(^4S)$	0.221	0.26±0.05 [d]	0.168	0.198±0.008	0.135	0.118±0.01	0.112	0.126±0.008
$2p^3(^2D)$	0.814	0.97±0.03 [e]	0.566	0.63±0.02	0.430	0.410±0.03	0.344	0.358±0.014
$2p^3(^2D)$				0.58±0.03				0.317±0.014
$2p^3(^2P)$	0.321	0.45±0.1 [e]	0.229	0.246±0.009	0.176	0.148±0.01	0.143	0.147±0.012
$2p^3(^2P)$				0.227±0.011				0.141±0.012

[a]Pinnington *et al.* [44].

[b]Knystautas *et al.* [46].

[c]Irwin, Livingston, and Kernahan [48].

[d]Bengtsson *et al.* [42].

[e]Berry *et al.* [36].

TABLE VII. Comparison of theoretical and experimental lifetimes (ps) for B-like ions with $Z=14-17$.

Level	Z=14 Present	Z=14 Expt. [a]	Z=15 Present	Z=15 Expt. [b]	Z=16 Present	Z=16 Expt.	Z=17 Present	Z=17 Expt. [c]
$2s2p^2(^2P_{1/2})$	63.7	58 ± 5	57.6	55 ± 6	52.6	81 [d]	48.6	58 ± 6
$2s2p^2(^2P_{3/2})$	62.5	58 ± 5	56.2		50.6	81 [d]	45.9	
$2s2p^2(^2S_{1/2})$	112	100 ± 8	99.2		88.0		77.9	80 ± 8
$2s2p^2(^2D_{3/2})$	469	490 ± 30	409	425 ± 30	359	380 ± 50 [e]	317	330 ± 30
$2s2p^2(^2D_{5/2})$	505	490 ± 30	450		405	410 [d]	368	
$2p^3(^4S_{3/2})$	66.3	59 ± 5	59.3		53.6	50 ± 10 [e]	48.7	53 ± 5
$2p^3(^2D_{3/2})$	183	175 ± 10	162		145	130 ± 10 [e]	130	
$2p^3(^2D_{5/2})$	182	175 ± 10	161		143	190 [d]	128	120 ± 10
$2p^3(^2P_{1/2})$	77.4	78 ± 5	68.8	73 ± 4	61.6		55.5	
$2p^3(^2P_{3/2})$	78.2	78 ± 5	69.6		62.4		56.2	55 ± 6

[a]Träbert and Heckmann [53].
[b]Träbert, Heckmann, and von Buttlar [51].
[c]Forester *et al.* [57].
[d]Pegg *et al.* [54].
[e]Träbert and Heckmann [55].

6 to 100. Our retarded E_1 matrix elements included correlation corrections from Coulomb and Breit interactions; contributions from negative energy states were also included to ensure gauge independence. Both length and velocity forms of the matrix elements were evaluated and small differences, caused by the nonlocality of the starting HF potential, were found between the two forms. Second-order MBPT transition energies were used in our evaluation of oscillator strengths and transition rates. These calculations were compared with other calculations and with available experimental data. For $Z\geq10$, we believe that the present theoretical data are more accurate than other theoretical or experimental data for transitions between $n=2$ states in B-like ions. We hope that these results will be useful in analyzing older experiments and planning new ones. Additionally, these calcu-lations provide basic theoretical input amplitudes for calculations of reduced matrix elements, oscillator strengths, and transition rates in four-valence atomic systems.

APPENDIX

The model space state vector for an ion with three valence electrons outside a closed core can be represented as [67]
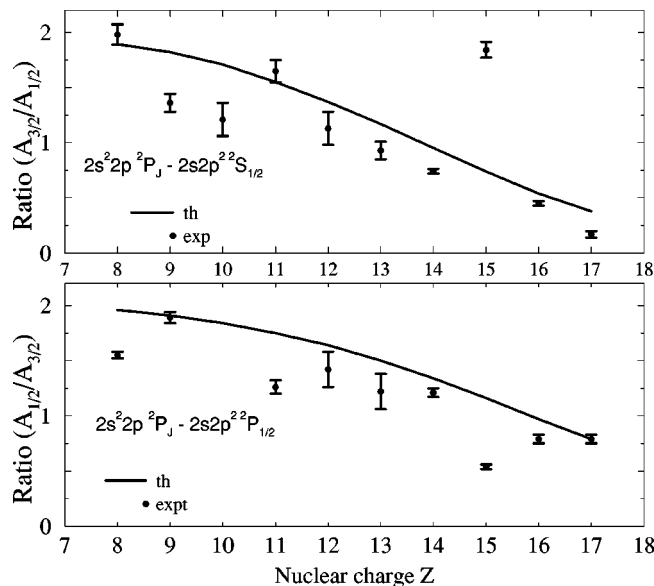

FIG. 3. Branching ratios: upper panel, $A_{3/2}/A_{1/2}$ for transitions $2s^22p\ ^2P_J - 2s2p^2\ ^2S_{1/2}$; lower panel, $A_{1/2}/A_{3/2}$ for transitions $2s^22p\ ^2P_J - 2s2p^2\ ^2P_{1/2}$. The experimental ratios are from Ref. [68].
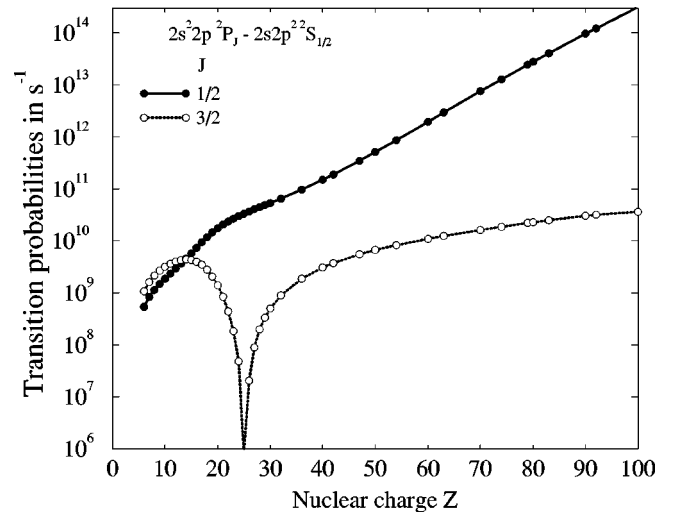

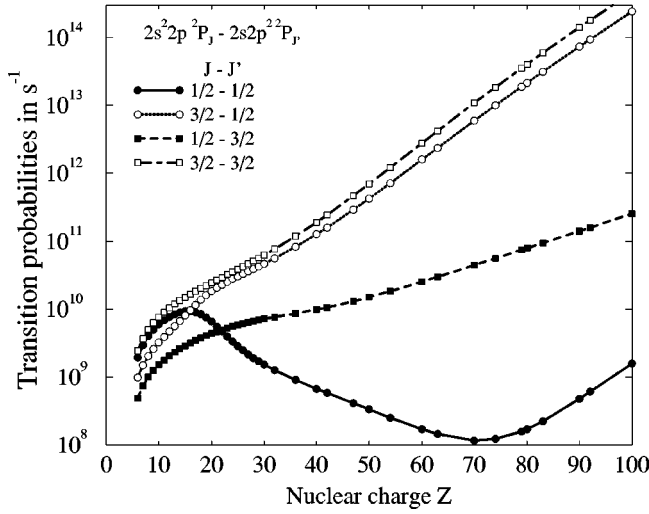FIG. 4. Rates for $2s^22p\ ^2P_{1/2,3/2} - 2s2p^2\ ^2S_{1/2}$ transitions as functions of Z.

FIG. 5. Rates for $2s^2 2p\ ^2P_{1/2,3/2} - 2s2p^2\ ^2P_{1/2,3/2}$ transitions as functions of Z.

FIG. 6. Rates for $2s^2 2p\ ^2P_{1/2,3/2} - 2s2p^2\ ^2D_{3/2,5/2}$ transitions as functions of Z.

$\Psi_0(v_1 w_1[J_{12}]u_1 JM)$

$$= \sum_{vwu} \sum_{K_{12}''} \langle vw|K_{12}''\rangle \langle K_{12}''u|K\rangle$$

$$\times C_{vv_1 ww_1 uu_1}(J_{12}, J_{12}'', J) a_v^\dagger a_w^\dagger a_u^\dagger |0\rangle, \qquad (A1)$$

where we use the notation $K_i = \{J_i, M_i\}$. Here $|0\rangle$ is the state vector for the core ($1s^2$, in our case). The quantity $\langle K_1 K_2|K_3\rangle$ is a Clebsch-Gordan coefficient:

$$\langle K_1 K_2|K_3\rangle = (-1)^{J_1 - J_2 + M_3}\sqrt{[J_3]}\begin{pmatrix} J_1 & J_2 & J_3 \\ M_1 & M_2 & -M_3 \end{pmatrix} \qquad (A2)$$

with $[J] = 2J + 1$. The quantity $C_{vv_1 ww_1 uu_1}(J_{12}, J_{12}'', J)$ is a symmetry coefficient defined in [67],

$C_{vv_1 ww_1 uu_1}(J_{12}, J_{12}'', J)$

$$= N(v_1 w_1[J_{12}]u_1)\Bigg[\delta(u, u_1)\delta(J_{12}, J_{12}'')P_{J_{12}}(vv_1, ww_1)$$

$$+ \delta(u, v_1)P_{J_{12}''}(vu_1, ww_1)\sqrt{[J_{12}][J_{12}'']}\begin{Bmatrix} u_1 & w_1 & J_{12}'' \\ v_1 & J & J_{12} \end{Bmatrix}$$

$$+ (-1)^{v_1 + w_1 + 1 + J_{12}}\delta(u, w_1)P_{J_{12}''}(vw_1, wv_1)$$

$$\times \sqrt{[J_{12}][J_{12}'']}\begin{Bmatrix} u_1 & v_1 & J_{12}'' \\ w_1 & J & J_{12} \end{Bmatrix}\Bigg], \qquad (A3)$$

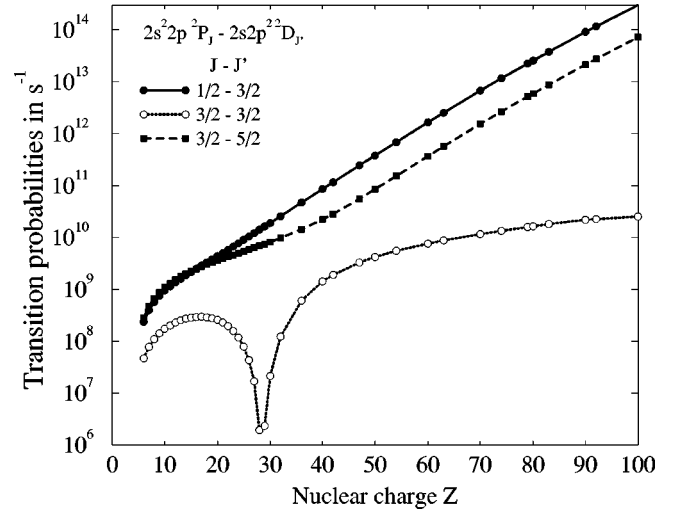where $N(v_1 w_1[J_{12}]u_1)$ is a normalization constant and

$$P_{J_{12}}(v_1 w_1, vw) = \delta_{v_1 v}\delta_{w_1 w} + (-1)^{j_v + j_w + J + 1}\delta_{w_1 v}\delta_{u_1 w}. \qquad (A4)$$

Using this representation, it is possible to express contributions in three-electron systems of first- and second-order MBPT diagrams in terms of the contributions of these diagrams to two-electron (berylliumlike) ions:

$Z^{(1+2)}(v_1 w_1(J_{12})u_1 J - v_2 w_2(J_{12}')u_2 J')$

$$= \frac{1}{2}\sum_{vwu}\sum_{v'w'}\sum_{J_{12}''J_{12}'''} Z^{(1+2)}(vwJ_{12}'' - v'w'J_{12}''')$$

$$\times S_{j_u}(J_{12}''J_{12}''', JJ')C_{vv_1 ww_1 uu_1}(J_{12}, J_{12}'', J)$$

$$\times C_{v'v_2 w'w_2 uu_2}(J_{12}', J_{12}''', J'), \qquad (A5)$$

where

$$S_j(J_{12}J_{12}', JJ') = (-1)^{j + J + J_{12}' + 1}\sqrt{[J][J']}\begin{Bmatrix} J & J' & 1 \\ J_{12}' & J_{12} & j \end{Bmatrix} \qquad (A6)$$

and

$$Z^{(1+2)}(vwJ - v'w'J') = Z^{(1)}(vwJ - v'w'J')$$

$$+ Z^{(RPA)}(vwJ - v'w'J')$$

$$+ 2Z^{(corr)}(vwJ - v'w'J'). \qquad (A7)$$

In the above equation, $Z^{(1)}$ is the uncoupled first-order E_1 matrix element for a two-electron system, while $Z^{(RPA)}$ and $Z^{(corr)}$ are random-phase approximation and correlation contributions to the uncoupled second-order matrix element for two-electron systems. The calculation of these matrix elements, which include contributions from the Coulomb and Breit interactions, was described previously in [66].

The second-order reduced matrix element of the derivative term is given by

$$Z^{(\mathrm{derv})}[\,vw(J_{12})uJ - v'w'(J'_{12})u'J'\,]$$

$$= \alpha[E^{(1)}_{vwu} - E^{(1)}_{v'w'u'}]$$

$$\times P^{(\mathrm{derv})}[\,vw(J_{12})uJ - v'w'(J'_{12})u'J'\,], \qquad (A8)$$

where $E^{(1)}_{vwu}$ is the first-order correction to the energy and α is the fine-structure constant. The quantity $P^{(\mathrm{derv})}$ in Eq. (A8) can be written in terms of its counterpart $P^{(\mathrm{derv})}(vwJ - v'w'J')$ in a two-electron system as

$$P^{(\mathrm{derv})}[\,v_1 w_1(J_{12})u_1 J - v_2 w_2(J'_{12})u_2 J'\,]$$

$$= \frac{1}{2} \sum_{vwu} \sum_{v'w'} \sum_{J''_{12}J'''_{12}} P^{(\mathrm{derv})}(vwJ''_{12} - v'w'J'''_{12})$$

$$\times S_{j_u}(J''_{12}J'''_{12},JJ') C_{vv_1ww_1uu_1}(J_{12},J''_{12},J)$$

$$\times C_{v'v_2w'w_2uu_2}(J'_{12},J'''_{12},J'). \qquad (A9)$$

Coupled three-particle matrix elements $Q^{(1+2)}(I-F)$ are given in terms of the uncoupled three-particle matrix elements discussed in the previous paragraphs by

$$Q^{(1+2)}(I-F)$$

$$= \frac{1}{E^I_1 - E^F_1} \sum_{vwu} \sum_{v'w'u'} C^I_1(vwu) C^F_1(v'w'u')$$

$$\times \{[\epsilon_{vwu} - \epsilon_{v'w'u'}] Z^{(1+2)}[\,vw(J_{12})uJ - v'w'(J'_{12})u'J'\,]$$

$$+ [E^I_1 - E^F_1 - \epsilon_{vwu} + \epsilon_{v'w'u'}]$$

$$\times P^{(\mathrm{derv})}[\,vw(J_{12})uJ - v'w'(J'_{12})u'J'\,]\}. \qquad (A10)$$

Here $\epsilon_{vwu} = \epsilon_v + \epsilon_w + \epsilon_u$ is the lowest-order energy; E^λ_1 with $\lambda = F$ or I is the first-order energy, which is given as the λth eigenvalue of the first-order effective Hamiltonian; and $C^\lambda_1(vwu)$ with $\lambda = F$ or I is the first-order coupling coefficient, which is given as the eigenvector belonging to E^λ_1. Using these formulas, we transform the uncoupled matrix elements between symmetrized jj states given in Table II to intermediate coupled matrix elements between physical states given in Table III.

[1] M. Cohen and A. Dalgarno, Proc. R. Soc. London, Ser. A **280**, 258 (1964).

[2] U. I. Safronova, A. N. Ivanova, and V. N. Kharitonova, Theor. Exp. Chem. **5**, 325 (1969).

[3] C. Laughlin and A. Dalgarno, Phys. Rev. A **8**, 39 (1973).

[4] U. I. Safronova and V. S. Senashenko, *Theory of Spectra of Multicharged Ions* (Energoatomizdat, Moscow, 1984).

[5] G. Merkelis, M. J. Vilkas, G. Gaigalas, and R. Kisielius, Phys. Scr. **51**, 233 (1995).

[6] P. Westhaus and O. Sinanoğlu, Phys. Rev. **183**, 56 (1969).

[7] O. Sinanoğlu and W. Luken, Chem. Phys. Lett. **20**, 407 (1973).

[8] O. Sinanoğlu, Nucl. Instrum. Methods **110**, 193 (1973).

[9] C. N. Nicolaides and D. R. Beck, J. Phys. B **6**, 535 (1973).

[10] O. Sinanoğlu and S. L. Davis, Chem. Phys. Lett. **32**, 449 (1975).

[11] O. Sinanoğlu and W. Luken, J. Chem. Phys. **64**, 4197 (1976).

[12] J. E. Hansen, J. Opt. Soc. Am. **59**, 722 (1969).

[13] R. Glass, J. Phys. B **13**, 15 (1980).

[14] R. Glass, J. Phys. B **13**, 899 (1980).

[15] D. H. Sampson, G. M. Weaver, S. J. Goett, H. Zhang, and R. E. H. Clark, At. Data Nucl. Data Tables **35**, 223 (1986).

[16] A. W. Weiss, Phys. Rev. **188**, 119 (1969).

[17] R. P. McEacharan and M. Cohen, J. Quant. Spectrosc. Radiat. Transf. **11**, 1819 (1971).

[18] L. J. Shamey, J. Opt. Soc. Am. **61**, 942 (1971).

[19] B. C. Fawcett, R. D. Cowan, and R. W. Hayes, Astrophys. J. **187**, 377 (1974).

[20] W. Dankwort and E. Trefftz, J. Phys. B **10**, 2541 (1977).

[21] W. Dankwort and E. Trefftz, Astron. Astrophys. **65**, 93 (1978).

[22] B. C. Fawcett, At. Data Nucl. Data Tables **22**, 473 (1978).

[23] K. D. Lawson, N. J. Peacock, and M. F. Stamp, J. Phys. B **14**, 1929 (1981).

[24] C. Froese Fischer, Phys. Scr. **49**, 323 (1994).

[25] T. Brage, C. Froese Fischer, and P. G. Judge, Astrophys. J. **445**, 457 (1995).

[26] Yu. Yan, K. T. Taylor, and M. J. Seaton, J. Phys. B **20**, 235 (1987).

[27] D. A. Verner, E. M. Verner, and G. J. Ferland, At. Data Nucl. Data Tables **64**, 1 (1996).

[28] H. Nussbaumer, Astrophys. J. **170**, 93 (1971).

[29] H. Nussbaumer and P. J. Storey, Astron. Astrophys. **71**, L5 (1979).

[30] A. Farrag, E. Luc-Koenig, and J. Sincelle, At. Data Nucl. Data Tables **24**, 227 (1979).

[31] A. Farrag, E. Luc-Koenig, and J. Sincelle, J. Phys. B **13**, 3939 (1980).

[32] K. T. Cheng, Y.-K. Kim, and J. P. Desclaux, At. Data Nucl. Data Tables **24**, 111 (1979).

[33] M. Vajed-Samii, D. Ton-That, and L. Armstrong, Jr., Phys. Rev. Lett. **23**, 3034 (1981).

[34] H. L. Zhang and D. H. Sampson, At. Data Nucl. Data Tables **56**, 221 (1994).

[35] L. Heroux, Phys. Rev. **153**, 156 (1967).

[36] H. G. Berry, W. S. Bickel, S. Bashkin, J. Désesquelles, and R. M. Schectman, J. Opt. Soc. Am. **61**, 947 (1971).

[37] J. P. Buchet, M.-C. Poulizac, and M. Carré, J. Opt. Soc. Am. **62**, 623 (1972).

[38] P. D. Dumont, E. Biemont, and N. Grevesse, J. Quant. Spectrosc. Radiat. Transf. **14**, 1127 (1974).

[39] P. D. Dumont, Y. Baudinet-Robinet, and A. E. Livingston, Phys. Scr. **13**, 365 (1976).

[40] K. Ishii, M. Suzuki, and J. Takahashi, J. Phys. Soc. Jpn. **54**, 3472 (1985).

[41] E. H. Pinnington, W. Ansbacher, R. N. Gosselin, and J. A. Kernahan, Phys. Lett. A **114**, 373 (1986).

[42] P. Bengtsson, L. J. Curtis, M. Henderson, R. E. Irving, and S.

T. Maniak, Phys. Scr. **52**, 507 (1995).

[43] I. Martinson, H. G. Berry, W. S. Bickel, and H. Oona, J. Opt. Soc. Am. **61**, 519 (1971).

[44] E. H. Pinnington, D. J. G. Irwin, A. E. Livingston, and J. A. Kernahan, Can. J. Phys. **52**, 1961 (1974).

[45] J. P. Buchet, M.-C. Buchet-Poulizac, and M. Druetta, J. Opt. Soc. Am. **66**, 842 (1976).

[46] E. Knystautas, M.-C. Buchet-Poulizac, J. P. Buchet, and M. Druetta, J. Opt. Soc. Am. **69**, 474 (1979).

[47] J. A. Kernahan, A. Denis, and R. Drouin, Phys. Scr. **4**, 49 (1971).

[48] D. J. G. Irwin, A. E. Livingston, and J. A. Kernahan, Can. J. Phys. **51**, 1948 (1973).

[49] J. A. Kernahan, K. E. Donnelly, and E. H. Pinnington, Can. J. Phys. **55**, 1310 (1977).

[50] J.-P. Buchet, M.-C. Buchet-Poulizac, and M. Druetta, Phys. Scr. **18**, 496 (1978).

[51] E. Träbert, P. H. Heckmann, and H. von Buttlar, Z. Phys. A **281**, 333 (1977).

[52] E. Träbert, P. H. Heckmann, W. Schlagheck, and H. von Buttlar, Phys. Scr. **21**, 27 (1980).

[53] E. Träbert and P. H. Heckmann, Phys. Scr. **21**, 35 (1980).

[54] D. J. Pegg, S. B. Elston, P. M. Griffin, H. C. Hayden, J. P. Forester, R. S. Thoe, R. S. Peterson, and I. A. Sellin, Phys. Rev. A **14**, 1036 (1976).

[55] E. Träbert and P. H. Heckmann, Phys. Scr. **22**, 489 (1980).

[56] K. Ishii, E. Alvarez, R. Hallin, J. Lindskog, A. Marelius, J. Pihl, R. Sjödin, B. Denne, L. Engström, S. Huldt, and I. Martinson, Phys. Scr. **18**, 57 (1978).

[57] J. P. Forester, D. J. Pegg, P. M. Griffin, C. D. Alton, S. B. Elston, H. C. Hayden, R. S. Thoe, C. R. Van, and J. J. Wright, Phys. Rev. A **18**, 1476 (1978).

[58] K. Kawatsura, M. Sataka, A. Ootuka, K. Komaki, H. Naramoto, K. Ozawa, Y. Nakai, and F. Fujimoto, Nucl. Instrum. Methods, Phys. Res. A **262**, 150 (1987).

[59] W. L. Wiese, J. R. Fuhr, and T. M. Deters, J. Phys. Chem. Ref. Data Monogr. **7**, 3 (1996).

[60] G. A. Martin, J. R. Fuhr, and W. L. Wiese, J. Phys. Chem. Ref. Data Suppl. **17**, Suppl. 3 (1988).

[61] T. Shirai, T. Nakagaki, J. Sugar, and W. L. Wiese, J. Phys. Chem. Ref. Data **21**, 273 (1992).

[62] T. Shirai, Y. Nakai, T. Nakagaki, J. Sugar, and W. L. Wiese, J. Phys. Chem. Ref. Data **22**, 1279 (1993).

[63] T. Shirai, T. Nakagaki, K. Okazaki, J. Sugar, and W. L. Wiese, J. Phys. Chem. Ref. Data **23**, 179 (1994).

[64] T. Shirai, Y. Funatake, K. Mori, J. Sugar, W. L. Wiese, and Y. Nakai, J. Phys. Chem. Ref. Data **19**, 127 (1990).

[65] T. Shirai, A. Mengoni, Y. Nakai, K. Mori, J. Sugar, W. L. Wiese, K. Mori, and N. Sakai, J. Phys. Chem. Ref. Data **21**, 23 (1992).

[66] U. I. Safronova, W. R. Johnson, M. S. Safronova, and A. Derevianko, Phys. Scr. **59**, 286 (1999).

[67] M. S. Safronova, W. R. Johnson, and U. I. Safronova, Phys. Rev. A **54**, 2850 (1996).

[68] J. Dörfert and E. Träbert, Phys. Scr. **47**, 524 (1993).

[69] See AIP Document No. E-PAPS:EPLRAAN-56-1268 for a table of lifetimes of $2s2p^2$ and $2p^3$ levels for boronlike ions with $Z = 6-100$ and a table of comparisons of transition rates and oscillator strengths with other theoretical data. E-PAPS document files may be retrieved free of charge from our FTP server (http://www.aip.org/pubservs/paps.html) or from ftp.aip.org in the directory /epaps/. For further information, e-mail: paps@aip.org or fax: 516-576-2223.